Characterization of the Resting Axolemma in the Giant Axon of the Squid

RAIMUNDO VILLEGAS and FLOR V. BARNOLA

From the Laboratorio de Biofísica, Instituto Venezolano de Investigaciones Científicas (I.V.I.C.), Caracas, Venezuela

ABSTRACT Previous electron microscope studies have shown that the Schwann cell layer is traversed by long and tortuous slit-like channels ~60Å wide, which provide the major route of access to the axolemma surface. In the present work the restriction offered by the resting axolemma to the passage of six small non-electrolyte molecules has been determined. The radii of the probing molecules were estimated from constructed molecular models. The ability of the axolemma to discriminate between the solvent (water) and each probing molecule was expressed in terms of the reflection coefficient σ. σ was then used to calculate an effective pore size for the resting axolemma. The value of 4.25 Å found for the pore radius is in excellent agreement with the 1.5 to 8.5 Å limiting values previously calculated from our measurements of water fluxes. The presence of pores with 4.25 Å radius in the resting axolemma is compatible with restricted diffusion of Na. The present paper leads to the conclusion that the axolemma is the only continuous barrier across which the ionic gradient responsible for the normal functioning of the nerve can be maintained. The combined findings of electron microscopy, water permeability, and molecular restricted filtration indicate that in all probability the axolemma is the "excitable membrane" of the physiologists.

Previous studies on the squid giant nerve fiber have shown agreement between the fine structure observed with the electron microscope (1–3) and the one suggested by the diffusion permeability coefficients of water (1, 2) and K^+ ions (4). The channels in the Schwann cell layer observed in high resolution electron micrographs appear as the common pathway for the ions and the water molecules to reach the axolemma surface. From the water permeability studies (1, 2) it was possible to determine the presence of pores in the axolemma with an effective radius between 1.5 Å and 8.5 Å.

The object of the present study is the determination of the reflection coeffi-

cient σ (5, 6) of the axolemma for a set of non-electrolytic molecules of small radii. σ describes the ability of the membrane to discriminate between the solvent and solute molecules. The σ values are then used (based on the principles developed by Durbin, Frank, and Solomon (7), Durbin (8, 9), and Solomon (10)) to calculate (*a*) an equivalent pore size, and (*b*) a geometrical pore area for the axon membrane in resting state.

EXPERIMENTAL METHOD

Principles

When an axon is immersed in a new environment, it is considered to be in transient osmotic equilibrium with it when the rate of volume change at zero time is zero; in this case the osmolarity of the new environment has balanced that of the axoplasm. In a medium containing only osmotically non-penetrating solutes an osmolarity of 1010 mOsM/liter is necessary to establish equilibrium with the axoplasm.[1] When only penetrating solutes are used outside, higher concentrations are needed to achieve osmotic balance at zero time. Preservation of nerve activity normally requires the presence of some inorganic ions, and therefore a partial substitution of the non-penetrating solutes by the penetrating solute has been made. The concentration of the penetrating solute required to balance a constant gradient of non-penetrating solutes is a function of the molecular radius of the permeable solute used.

Experimental Procedure

The giant nerve fiber from the first stellar nerve of the tropical squid *Doryteuthis plei* was used. The experiment consisted of determining the change in volume of the axon as a function of time after its artificial sea water environment was replaced by a test solution. The technique and equipment were the same as those previously described (*cf.* reference 1). The isolated nerve fibers are placed along specially made lucite holders containing isotonic sea water. They are kept slightly under tension by means of threads tied at both ends. The length was measured with 0.1 mm. precision with a vernier micrometer. The axon diameter was measured with a microscope equipped with an ocular micrometer, the divisions of which were standardized by a Zeiss stage micrometer. Each division of the ocular micrometer corresponded to 5.0×10^{-4} cm. and the image was sufficiently sharp to permit measurements with a precision of a third of a scale division. The objective was immersed in the sea water, care being taken to avoid nerve fiber compression. The axon diameter was measured at consecutive intervals of approximately 10 sec. from the time of immersion of the

[1] In the present paper non-penetrating solutes are considered the normal constituents of artificial sea water and the axoplasm (*cf.* reference 1). Penetrating solutes are those for which the axolemma behaves as a non-selective membrane. The fraction of cell water which is apparently free to participate in the osmotic phenomena has already been determined (1).

nerve in the test solution, the timing error being approximately ±1 sec. At the end of the observation period the test solution was replaced by isotonic artificial sea water; the fiber then returned to its initial diameter. Three different test solutions with varying concentrations of the same penetrating solute were used in each experiment. The order in which they were applied to the nerve, corresponds to that shown in Table I, from (*a*) to (*d*). Each test solution remained in contact with the tissue for a maximum time of 2 minutes. The nerve was immersed in the isotonic artificial sea water for 10 minutes between observation periods, and the sea water was replaced at least twice during this interval in order to remove any remaining traces of the previous solution. Experiments were carried out at 22–24°C.

TABLE I

CONCENTRATION OF TEST SOLUTES IN THE BATHING FLUID

Solute	(*a*) Concentration	(*b*) Concentration	(*c*) Concentration	(*d*) Concentration
	mOsm/liter	*mOsm/liter*	*mOsm/liter*	*mOsm/liter*
Methanol	230	65	140	—
Formamide	230	50	118	—
Ethanol	230	65	—	479
Urea	230	60	—	479
Ethylene glycol	230	55	—	479
Glycerol	230	60	—	394

Results were accepted as valid when (*a*) microscopic alteration of the structure was not appreciable; and (*b*) a normal action potential was evoked upon electrical stimulation at the end of the experiment. In order to maintain the normal resting state no other electrical stimulation was applied to the fibers. No changes have been observed in the axon diameter during 1 hour exposure to isotonic sea water.

Composition of the Solutions

Artificial sea water as described by Hodgkin and Katz (11), was used as a normal medium. The concentration of its components in millimols per liter was as follows: NaCl, 441.7; KCl, 9.9; $CaCl_2 \cdot 2H_2O$, 11.0; $MgCl_2 \cdot 6H_2O$, 53.1; $NaHCO_3$, 2.5. Its osmolarity of 1010 mOsM/liter was taken as isosmolar with the axoplasm.

Test solutions were made with artificial sea water from which 230 milliosmols of NaCl per liter had been removed, giving a final osmolarity of 780 mOsM/liter. Different amounts of a single non-electrolyte were then added to obtain the concentrations shown in Table I. The solutes used were methanol, formamide, ethanol, urea, ethylene glycol, or glycerol. The osmolarities given in the text and tables were measured with a freezing point osmometer (Fiske osmometer apparatus) with an accuracy of ±1 mOsM/liter. The cryoscopic point of a solution that has a concentration of 1 osmol per kg. of water is −1.858°C.

Molecular Radii

The radii of the probing molecules were estimated from constructed molecular models and their dimensions measured with a precision of 0.1 mm. by means of a vernier micrometer. In the Fisher-Hirschfelder-Taylor atom models used, 1 cm. is equivalent to 1 Å. The molecular model was orientated to give the smallest possible configuration, and its dimensions along three perpendicular axes determined. The measurements were repeated with a molecular model giving the largest possible configuration. The radius was taken as $r_s = 0.5[0.5\sqrt[3]{d_{1l}\, d_{2l}\, d_{3l}} + 0.5\sqrt[3]{d_{1s}\, d_{2s}\, d_{3s}}]$,

TABLE II

MOLECULAR RADIUS OF THE TEST SOLUTES

Solute	Radius in Å ± S.E.
Methanol	1.83+0.002
Formamide	1.96±0.02
Ethanol	2.13±0.02
Urea	2.17±0.01
Ethylene glycol	2.24±0.01
Glycerol	2.77±0.03

in which d_{il} and d_{is} are the diameters of the model for the largest and smallest configurations respectively. Five determinations of r_s were made for each molecule and the mean ± standard error is shown in Table II. The radius of the water molecule was taken as 1.5 Å (12).

MATHEMATICAL TREATMENT

The net volume flow per unit area[2] in the absence of an hydrostatic pressure gradient, for the case of a system composed of a membrane permeable to solvent and to one probing non-ionic solute, and impermeable to the other solutes present, is described by the following equation:

$$J_v = L_p\, \Delta\pi_i - \sigma L_p RT \Delta c_s \qquad (1)$$

in which the symbols have the following meaning:

J_v = the net volume flow per unit area, equal to dV/Adt, V being the axon volume, A the area, and t the time,

L_p = the phenomenological coefficient,

$\Delta\pi_i$ = the osmotic pressure difference across the membrane produced by non-penetrating solutes,

[2] The area of the nerve is assumed to remain constant. Due to the irregularities in the axon surface in isotonic sea water the cell may begin to swell with no changes in its area. It should be pointed out that the present method of determining the equivalent pore radius is based upon measurements of the initial rate of volume change.

R = the gas constant,
T = the absolute temperature,
Δc_s = the concentration difference of penetrating solute across the membrane; *i.e.*, the concentration of the test solute in the bathing fluid assuming the absence of penetrating solutes in the cell interior,
σ = the Staverman reflection coefficient (5, 6). The limiting values of this coefficient are: (*a*) $\sigma = 1$ in the case of an ideally selective membrane, and (*b*) $\sigma = 0$ when the solvent and solute pass across the membrane with equal velocity.

Utilizing the approach of Kedem and Katchalsky (13) Equation 1 was derived (Appendix I) and is related to their Equation 39

Hence from Equation 1:

$$\sigma = (\Delta\pi_i/RT)/\Delta c_s, \quad \text{when} \quad J_v = 0 \quad \text{at} \quad t = 0 \tag{2}$$

In the present experiments the concentration differences of non-penetrating and penetrating solutes, $\Delta\pi_i/RT$ and Δc_s, respectively, are expressed in osmolar units.

Durbin, Frank, and Solomon (7) have suggested, and later Durbin (8, 9) has demonstrated that:

$$\sigma = 1 - A_{sf}/A_{wf} \tag{3}$$

in which A_{sf}, and A_{wf} are the effective pore areas available for the passage of solute and solvent molecules respectively.

A_{xf}, the effective pore area for filtration of any molecule x passing through a membrane, is given by Renkin's Equation 19 (14):

$$A_{xf} = A_p\left[2\left(1 - \frac{r_x}{r_p}\right)^2 - \left(1 - \frac{r_x}{r_p}\right)^4\right]$$
$$\left[1 - 2.104\left(\frac{r_x}{r_p}\right) + 2.09\left(\frac{r_x}{r_p}\right)^3 - 0.95\left(\frac{r_x}{r_p}\right)^5\right] = A_p f\left(\frac{r_x}{r_p}\right) \tag{4}$$

in which A_p is the geometrical pore area, r_x the radius of the molecule, and r_p the pore radius. The ratio A_{sf}/A_{wf} can be determined for any chosen value of r_p by substituting in Equation 4 numerical values of r_x for a given solute and water:

$$A_{sf}/A_{wf} = f(r_s/r_p)/f(r_w/r_p) \tag{5}$$

in which r_s and r_w are the molecular radii of any solute and water respectively. Then, from Equations 3 and 5:

$$\sigma = 1 - [f(r_s/r_p)/f(r_w/r_p)] \tag{6}$$

To determine the equivalent pore size of the axolemma, a family of theoretical curves was calculated from Equation 6 for r_p values of 1.5 to 8.5 Å in steps of 0.25 Å. In the curves values for $1 - \sigma$ are plotted as a function of the molecular radii. The experimental values of $1 - \sigma$ calculated from Equation 2 are juxtaposed to the best fitting theoretical curve.

RESULTS AND DISCUSSION

The Equivalent Pore Size

Axon volume changes per unit area in formamide test solution, are shown in Fig. 1. Fig. 2 shows the initial rate of volume change per unit area, in the region where $t \rightarrow 0$, as a function of Δc_s for a constant concentration difference of non-penetrating solutes, $\Delta\pi_i/RT$, of 230 mOsM/liter. As shown in Fig. 2, the concentration of penetrating solute which gives zero rate of volume change at zero time decreases with increasing molecular radius. The results

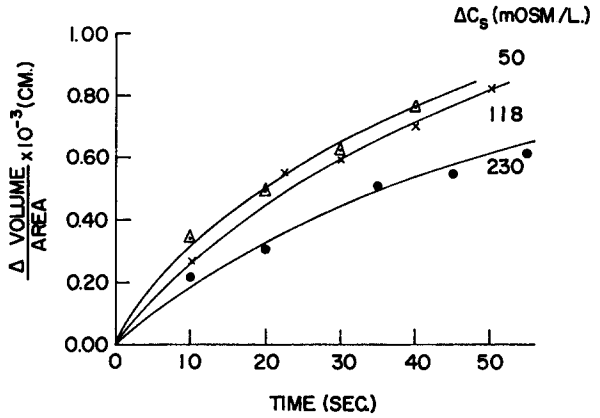

FIGURE 1. The squid giant axon volume changes per unit area in formamide test solutions plotted as a function of time. The initial slope of the curves represents the rate of volume change at a time near to zero when the penetration of the probing solutes to the membrane phase is negligible. $\Delta\pi_i/RT$ = 230 mOsM/liter.

for twenty-eight axons, and a total of six test solutes are summarized in Table III. When the value of $\Delta\pi_i/RT$ is divided by the corresponding Δc_s for zero rate of volume change at a time close to zero, the reflection coefficient σ can be calculated (Equation 2). The values of σ and $1 - \sigma$ are presented in Table IV. In Fig. 3, the average $(1 - \sigma) \pm$ one standard error is plotted as a function of the molecular radii. The continuous line in Fig. 3, represents the theoretical curve describing most closely the experimental results. It corresponds to an equivalent pore size of 4.25 Å, while the uncertainty in fitting the curve is ± 0.25 Å.

The adequacy of mixing the test solution with the extracellular space fluid cannot be measured experimentally, but may be estimated by calculation. It is possible to approximate diffusion in the extracellular space, if this space is considered as a plane liquid sheet covering the axon. Since diffusion between the extracellular space and the bathing solution occurs only across a single boundary of the plane, the calculation may be accomplished by using

Equation 2 of reference 1, with a thickness set at double the actual thickness of the extracellular space.[3] Electron micrographs of a group of nerves similarly dissected and cleaned of surrounding tissue, show that the connective tissue

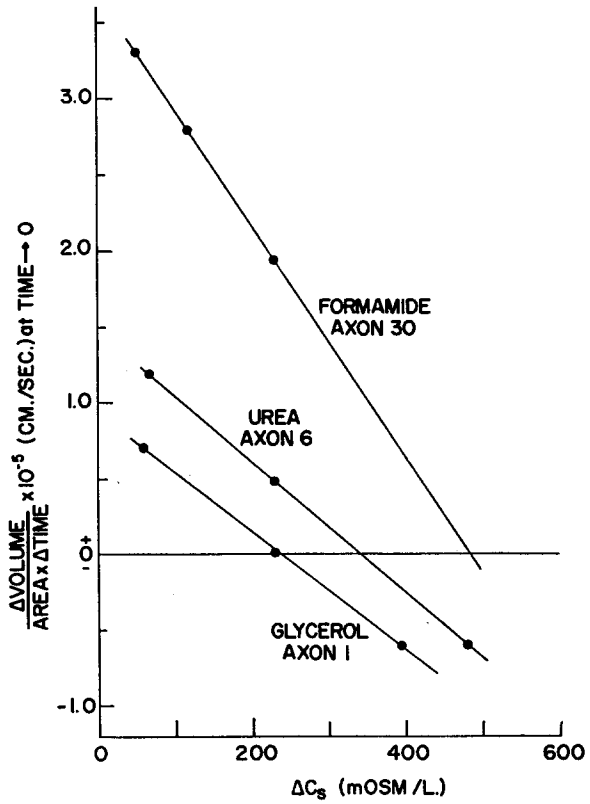

FIGURE 2. The initial rate of volume change per unit area, plotted as a function of the concentration of penetrating solutes in the test solutions, for a constant concentration difference of osmotically non-penetrating solutes. It is shown that the amount of permeable solute necessary to establish osmotic balance is a function of the molecular radius of the penetrating solute used. $\Delta\pi_i/RT = 230$ mOSM/liter.

around the nerve in the present experiments is a layer no thicker than 2 μ. The diffusion coefficient of the solute is assumed to be equal to that in ordinary

[3] Equation 2 of reference 1 is:

$$\frac{c}{c_0} = 1 - \frac{8}{\pi^2} e^{-(D\pi^2/4b^2)t}$$

in which c/c_0 is the ratio of the concentration of the test solute in the extracellular space to that in the bathing fluid, D is the diffusion coefficient of the solute, and b the half thickness of the extracellular space. It should be noted that this equation applies equally to the case of the solute diffusing in or diffusing out of a plane sheet. The change from any preexisting conditions is expected to follow the course predicted by this equation. The equation can be employed with any diffusion constant.

water; in the case of glycerol it is 0.82×10^{-5} cm.^{2}/sec. for a 228 mM/liter concentration at 20°C. as obtained by graphical interpolation from International Critical Tables (15). Under these conditions the extracellular solute

TABLE III

CONCENTRATION DIFFERENCE OF TEST SOLUTES (Δc_s) WHICH BALANCE A 230 *m*OSM/LITER DIFFERENCE OF NON-PENETRATING SOLUTES ($\Delta \pi_i$/RT) AT ZERO TIME

Temperature 22–24°C.

Solute	Axon No.	Axon diameter	Δc_s
		μ	*mOsm/liter*
Methyl alcohol	11	248	762
	13	303	880
	14	177	622
	15	196	766
	26	269	656
	27	265	700
	28	184	450
Formamide	29	284	583
	30	196	485
	31	319	545
	32	246	480
	33	284	593
Ethyl alcohol	16	196	336
	17	167	368
	18	154	327
	19	273	390
	20	255	418
Urea	5	220	334
	6	260	340
	7	234	296
	9	255	350
Ethylene glycol	10	243	316
	24	339	348
	25	316	298
Glycerol	1	393	230
	2	243	240
	3	360	240
	4	256	252

concentration would reach 90 per cent of that in the bathing solution within 3×10^{-3} sec. Since the first measurement of the volume change was recorded after a 10 sec. interval, diffusion in the extracellular space does not appear to affect the experimental observations.

TABLE IV

REFLECTION COEFFICIENT σ, OF THE AXOLEMMA FOR THE TEST SOLUTES

Solute	Axon No.	σ	$1 - \sigma$
Methyl alcohol	12	0.30	0.70
	13	0.26	0.74
	14	0.37	0.63
	15	0.30	0.70
	26	0.35	0.65
	27	0.33	0.67
	28	0.51	0.49
Average ± S.E.		0.35±0.03	0.65±0.03
Formamide	29	0.43	0.57
	30	0.47	0.53
	31	0.42	0.58
	32	0.48	0.52
	33	0.39	0.61
Average ± S.E.		0.44±0.02	0.56±0.02
Ethyl alcohol	16	0.68	0.32
	17	0.62	0.38
	18	0.70	0.30
	19	0.59	0.41
	20	0.55	0.45
Average ± S.E.		0.63±0.03	0.37±0.03
Urea	5	0.69	0.31
	6	0.68	0.32
	7	0.78	0.22
	9	0.66	0.34
Average ± S.E.		0.70±0.03	0.30±0.03
Ethylene glycol	10	0.73	0.27
	24	0.66	0.34
	25	0.77	0.23
Average ± S.E.		0.72±0.03	0.28±0.03
Glycerol	1	1.00	0.00
	2	0.96	0.04
	3	0.96	0.04
	4	0.91	0.09
Average ± S.E.		0.96±0.02	0.04±0.02

Since both the Schwann cell and the axolemma lie between the extracellular space and the axoplasm, it is important to demonstrate that the axolemma is the barrier to which the present measurements refer. When a molecule such as glycerol, with a radius of 2.77 Å, passes through a cylindrical pore 60 Å in diameter, the reflection coefficient σ can be calculated to be 0.10. The Schwann cell channels are not cylindrical pores but slits ~60 Å wide. Fric-

tion, during passage, is important along one dimension only, thus the calculated σ can only be regarded as an upper limit and the assumption that the axolemma is the barrier across which the net volume flow measured takes place is apparently justified. The concentration gradient across the Schwann cell layer will disappear as soon as the concentration in the axon–

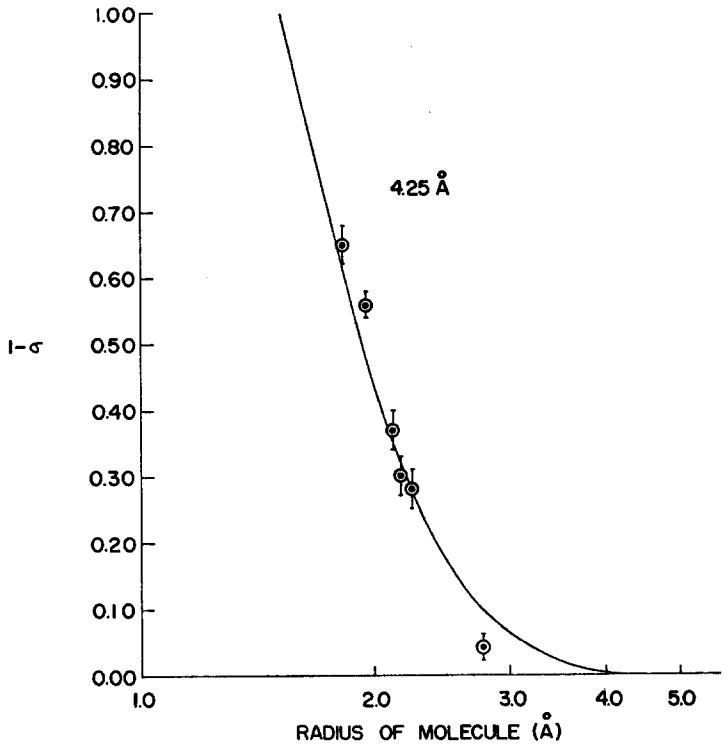

FIGURE 3. Experimental values of $(1 - \sigma) \pm$ standard error, for the squid nerve axolemma, plotted as a function of the molecular radius. These values are fitted by a theoretical curve corresponding to an equivalent pore radius of 4.25 Å. The uncertainty in fitting the curve is $\pm$ 0.25 Å.

Schwann cell space ~83 Å wide becomes equal to the external solution. It is possible to show that a solute present in the bathing fluid diffuses into the axon–Schwann cell space according to the following equation:

$$c = c_i[1 - e^{-(D_s A/\Delta x v)t}] \qquad (7)$$

in which:

c = the concentration of the solute in the axon–Schwann cell space,
c_i = the concentration of the solute in the bathing fluid,

D_s = the diffusion coefficient of the solute through the channels, assumed to be equal to that in ordinary water; in the case of glycerol it is 0.82×10^{-5} cm.^{2}/sec. for a 228 mM/liter concentration at 20°C. (15),

A = the area for diffusion of the solute, taken as that for water (minimum value 0.23 per cent of the Schwann cell surface), times 0.94 which represents the glycerol restriction to diffusion relative to water through slits 60 Å wide (16),[4]

Δx = the diffusion channel length which is taken as 4.3 μ (1),

v = the volume of the axon–Schwann cell space; for a 1 cm. segment of the nerve, with an axon diameter of 300 μ, the computed value of v is 3.86×10^{-8} cm.^{3},

t = the time in seconds.

Upon introducing these values in Equation 7 one obtains $t = 10^{-2}$ sec.; the time for the axon–Schwann cell space concentration to attain 90 per cent of the bathing fluid concentration. In these experiments the first observation was made at approximately 10 sec. after submersion of the nerve in the test solution; *i.e.*, the axon–Schwann cell space solution was equal to that of the test solution considerably before the moment of the first experimental observation.

The deviations of the experimental points from the theoretical curve, which are observed in Fig. 3, may be related to the simplification involved in the estimation of the molecular radii. In general, substances containing polar groups, such as —OH, and —NH_2, which have a tendency to form chemical linkages with the water molecules, are expected to have an effective radius larger than that obtained from measurements of their molecular models. Thus, glycerol, with three —OH groups would be expected, in the present set of molecules, to show the largest difference. The value for the radius of the glycerol molecule (2.77 Å) as obtained from the molecular model measurements, is in good agreement with the value of 2.90 Å determined by Schultz and Solomon (17) for the hydrated glycerol molecule. Hence, the ± 0.25 Å tolerance with which the experimental data and the theoretical curve are fitted is assumed to cover the uncertainty in the estimation of the molecular radii.

It should be noted that the present method of determining the equivalent pore size is based on experimental measurements taken at a time near zero when the penetration of the probing solutes through the membrane would be negligible. This is supported by the fact that the data do not show a correlation between values of σ and the respective oil-water partition coefficients.

[4] Pappenheimer *et al.* (reference 16, Equation 11) give the following equation to calculate the restriction to diffusion of spherical molecules through slit:

$$D_{\text{restricted}}/D_{\text{free}} = [1 - (r_s/0.5w)]/[1 + 3.4(r_s/0.5w)^2],$$

in which r_s is the radius of the penetrating molecule, and $0.5w$ is the slit half-width.

The oil-water partition coefficients of formamide, urea, ethylene glycol, and glycerol are less than 0.001; the methanol and ethanol coefficients have values of 0.009 and 0.036 respectively, as obtained by graphical interpolation from Collander and Barlund's data as presented by Höber (18).

The Geometrical Pore Area

An estimate of A_p, the geometrical pore area per cm.^{2} of axolemma, may be obtained if P_{da} (the water diffusion permeability coefficient of this membrane), and the equivalent pore radius are known. The presence of the slit-like channels in the Schwann cell precluded, as previously noted (1), the direct measurement of P_{da}. It is possible to calculate P_{da} by combining P_w (the water filtration permeability coefficient of this membrane) and its equivalent pore radius. If it is assumed that the diffusion of water through the pores may be described by Fick's law, and the osmotic flow of water by Poiseuille's law, then from Equations 21 and 22 of Paganelli and Solomon (19) we have:

$$r_p = -r_w + \sqrt{2r_w^2 + \lambda} \tag{8}$$

$$\lambda = (r_p + r_w)^2 - 2r_w^2 = [P_w - (P_{da}/\Delta a_w]8\eta D_{H_2O}/P_{da} \tag{9}$$

and solving for P_{da} gives:

$$P_{da} = \frac{P_w 8\eta D_{H_2O} \Delta a_w}{\lambda \Delta a_w + 8\eta D_{H_2O}} \tag{10}$$

In these equations η is the viscosity of water, whose value is 9.36×10^{-3} poise at 23°C.; D_{H_2O} is taken as the diffusion coefficient of $H^1{}_2O^{18}$ at 23°C.; *i.e.*, 2.65×10^{-5} cm.^{2}/sec. (20); and Δa_w is the difference in water activity across the membrane when an unidirectional flux of labeled water is measured. The activity gradient for the diffusion of water is 55.2 moles/liter which is equivalent to 1.38×10^6 cm. water pressure at 23°C. P_w for the axolemma is 7.8×10^{-10} ml. H_2O/(cm.^{2}, sec., cm. H_2O pressure) (1). Substitution of these values in Equation 10 yields $P_{da} = 3.60 \times 10^{-4}$ ml. H_2O/sec., cm.^{2} of the axolemma.

A_{pd}, the effective pore area for water diffusion per cm.^{2} of axolemma, is obtained from the expression $P_{da}/D_{H_2O} = A_{pd}/\Delta x$. The present experiments give a value of $A_{pd}/\Delta x = 13.6$ cm. per cm.^{2} of axolemma. For $\Delta x = 79$ Å, assuming the diffusion path length to be equal to the axolemma thickness as estimated from electron micrograph measurements (1, 3), $A_{pd} = 1.1 \times 10^{-5}$ cm.^{2} per cm.^{2} of axon membrane. From Renkin's Equation 11, A_p, the geometrical pore area, is given by:

$$A_p = A_{pd} \Big/ \left\{ \left(1 - \frac{r_w}{r_p}\right)^2 \left[1 - 2.104\left(\frac{r_w}{r_p}\right) + 2.09\left(\frac{r_w}{r_p}\right)^3 - 0.95\left(\frac{r_w}{r_p}\right)^5\right]\right\} \tag{11}$$

Substitution of A_{pd}, r_w, and r_p, in Equation 11 gives $A_p = 7.6 \times 10^{-5}$ cm.^{2} of pore area per cm.^{2} of axolemma. Assuming the axon membrane to be perforated by an homogeneous population of right cylindrical pores of 4.25 Å radius, it can be calculated that there are 1.3×10^{10} pores per cm.^{2} of axolemma. This idealized geometrical picture should be regarded as a computational device rather than a structural reality.

Hodgkin and Keynes (21) and Hodgkin (22) have considered the possible existence of two fundamental mechanisms for transport of ions in the nerve. In parallel with a pore system, which would allow ions to move passively through the membrane, an active transport mechanism might be present which would absorb potassium and extrude sodium against the electrochemical potential gradient. The proposed active transport system, made up of carrier molecules driven by metabolic energy, is related to the maintenance of the steady state ionic concentration gradient and to the recovery process (21–24). The downhill ionic movements, both in the resting membrane and those accompanying the action potential, would occur through the pores. It is tempting to assume a possible relation between the pores in the excitable membrane proposed by Hodgkin and Keynes (21) and those found in the axolemma herein described. Tobias' (25, 26) recent results seem to indicate that the ionic discrimination is apparently related to the lipid components of the excitable membrane. Taking the axolemma thickness, and even that of the lipid layers, as the minumum length of the pores, it may be observed that the path dimensions agree with the hypothesis of single file diffusion of potassium across the membrane phase (27). Mullins (28–31) has further assumed a Gaussian pore radius distribution to explain the membrane permeability coefficients for the different ions. Since it appears improbable that unhydrated ions could be present in appreciable quantities at room temperature, he suggested that the hydration shells exceeding the path diameter are replaced with a solvation of similar magnitude by the adjacent pore wall molecules during the journey. For the solvation from the pore wall to be at all effective, it must fit the ion closely; therefore, if the pore is too large the ion will be excluded. At the present time no experimental evidence is available concerning the passing of ions through pores in the axolemma.

The value of 4.25 Å found for the effective pore radius in the axolemma is independent of the nature of the hypothesis used to explain the ion transport mechanism. However, this value is wholly compatible with the controlled ionic environment responsible for the normal functioning of the nerve (22).

Our thanks are due to Dr. A. K. Solomon for helpful discussions during his stay in our laboratory; to Dr. Guillermo Whittembury, Dr. Richard P. Durbin, Dr. Leon McPherson, Dr. Leopoldo Villegas, and Dr. Julian M. Tobias for reading the manuscript and for their helpful suggestions. We are indebted to Mr. E. Jungo for his technical assistance.

APPENDIX I

Kedem and Katchalsky (13) have defined J_v, the net volume flow per unit area, and J_D, the relative velocity of solute *versus* solvent, for a system composed of solvent, non-ionic solute, and membrane, permeable to both solute and solvent, by the following equations:

$$J_v = L_p\Delta p + L_{pD}RT\Delta c_s \tag{1a}$$

$$J_D = L_{Dp}\Delta p + L_DRT\Delta c_s \tag{2a}$$

$$L_{pD} = L_{Dp} \tag{3a}$$

The symbols in these equations are defined as follows: $J_v = \dot{n}_w\bar{v}_w + \dot{n}_s\bar{v}_s$, in which $\dot{n}_w$ and $\dot{n}_s$ are the corresponding solvent and solute flows in moles per second per unit area; $\bar{v}_w$ and $\bar{v}_s$ are the partial molar volumes of solvent and solute respectively; $J_D = (\dot{n}_s/c_s) - (\dot{n}_w/c_w)$, in which c_s and c_w are the corresponding concentrations of solute and solvent; L_p, L_D = direct coefficients; L_{Dp}, L_{pD} = cross-coefficients; Δp = the hydrostatic pressure difference across the membrane; R = the gas constant; T = the absolute temperature; Δc_s = the concentration difference of permeable solutes.

In the case in which the membrane is impermeable to the solute, $J_v = \dot{n}_w\bar{v}_w$, and $J_D = -(\dot{n}_w/c_w)$. Since $c_w = 1/\bar{v}_w$ for dilute solutions, it can be concluded that $J_v = -J_D$ for an ideal semipermeable membrane. In this case:

$$(L_p + L_{pD})\Delta p + (L_D + L_{pD})RT\Delta c_s = 0 \tag{4a}$$

$$L_p + L_{pD} = L_D + L_{pD} = 0 \tag{5a}$$

$$L_p = -L_{pD} = L_D \tag{6a}$$

Equations 4 *a* and 6 *a* are also due to Kedem and Katchalsky (reference 13, their Equations 23 and 24). For a non-selective membrane, $-L_{pD} < L_p$, Staverman's (5, 6) reflection coefficient is introduced making $-L_{pD} = \sigma L_p$. Substituting for $-L_{pD}$ in Equation 1 *a*:

$$J_v = L_p\Delta p - \sigma L_pRT\Delta c_s \tag{7a}$$

The hydrostatic pressure difference, Δp, can be equated to an osmotic pressure gradient $\Delta\pi_i$, produced by non-penetrating solutes (8, 9). Substituting Δp in Equation 7 *a* gives:

$$J_v = L_p\Delta\pi_i - \sigma L_pRT\Delta c_s \tag{8a}$$

Equation 8 *a* describes J_v, for the case of a system composed of a membrane permeable to solvent, and to one probing non-ionic solute present in one side, and impermeable to the other solutes present, in the absence of an hydrostatic pressure gradient.

Received for publication, August 12, 1960.

BIBLIOGRAPHY

1. VILLEGAS, R., and VILLEGAS, G. M., *J. Gen. Physiol.*, 1960, **43**, No. 5, suppl., 73.
2. VILLEGAS, R., and VILLEGAS, G. M., *in* 2nd Interamerican Symposium on the Peaceful Application of Nuclear Energy, Buenos Aires, 1959, Washington, D. C., Organization of the American States, 1960, 77.
3. VILLEGAS, G. M., and VILLEGAS, R., *J. Ultrastructure Research*, 1960, **3**, 362.
4. FRANKENHAEUSER, B., AND HODGKIN, A. L., *J. Physiol.*, 1956, **131**, 341.
5. STAVERMAN, A. J., *Rec. trav. chim. Pays-bas*, 1951, **70**, 344.
6. STAVERMAN, A. J., *Rec. trav. chim. Pays-bas*, 1952, **71**, 623.
7. DURBIN, R. P., FRANK, H., and SOLOMON, A. K., *J. Gen. Physiol.*, 1956, **39**, 535.
8. DURBIN, R. P., Proceedings of the First National Biophysics Conference, New Haven, Yale University Press, 1959, 323.
9. DURBIN, R. P., *J. Gen. Physiol.*, 1961, **44**, 315.
10. SOLOMON, A. K., *J. Gen. Physiol.*, 1960, **43**, No. 5, suppl., 1.
11. HODGKIN, A. L., and KATZ, B., *J. Physiol.*, 1949, **108**, 37.
12. MORGAN, J. R., and WARREN, B. E., *J. Chem. Physics*, 1938, **6**, 666.
13. KEDEM, O., and KATCHALSKY, A., *Biochim. et Biophysica Acta*, 1958, **27**, 229.
14. RENKIN, E. M., *J. Gen. Physiol.*, 1954, **38**, 225.
15. International Critical Tables, National Research Council, New York, McGraw-Hill Book Co., 1928, **5**, 70.
16. PAPPENHEIMER, J. R., RENKIN, E. M., and BORRERO, L. M., *Am. J. Physiol.*, 1951, **167**, s13.
17. SCHULTZ, S. G., and SOLOMON, A. K., Abstracts of the Fourth Annual Meeting of the Biophysical Society, Philadelphia, 1960, 14.
18. HÖBER, R., Physical Chemistry of Cells and Tissues, Philadelphia, The Blakiston Co., 1945, 232.
19. PAGANELLI, C. V., and SOLOMON, A. K., *J. Gen. Physiol.*, 1957, **41**, 259.
20. WANG, J. H., ROBINSON, C. V., and EDELMAN, I. S., *J. Am. Chem. Soc.*, 1953, **75**, 466.
21. HODGKIN, A. L., and KEYNES, R. D., *J. Physiol.*, 1955, **128**, 28.
22. HODGKIN, A. L., *Proc. Roy. Soc. London, Series B*, 1957, **148**, 1.
23. CALDWELL, P. C., and KEYNES, R. D., *J. Physiol.*, 1957, **137**, 12P.
24. HODGKIN, A. L., (CALDWELL, P. C., KEYNES, R. D., SHAW, T. I., and HODGKIN, A. L.) Symposia on Ionic Transmission Across Membranes. XXI, International Congress of Physiological Sciences, Buenos Aires, 1959, 168.
25. TOBIAS, J. M., *J. Cell. and Comp. Physiol.*, 1958, **52**, 89.
26. TOBIAS, J. M., *J. Gen. Physiol.*, 1960, **43**, No. 5, suppl., 57.
27. HODGKIN, A. L., and KEYNES, R. D., *J. Physiol.*, 1955, **128**, 61.
28. MULLINS, L. J., *in* Molecular Structure and Functional Activity of Nerve Cells, (R. G. Grenell and L. J. Mullins, editors), Washington, D. C., American Institute of Biological Sciences, Symposium No. 1, 1956, 123.
29. MULLINS, L. J., *J. Gen. Physiol.*, 1959, **42**, 817.
30. MULLINS, L. J., *J. Gen. Physiol.*, 1959, **42**, 1013.
31. MULLINS, L. J., *J. Gen. Physiol.*, 1960, **43**, No. 5, suppl., 105.